Bulgarian Chemical Communications, Volume 46, Special Issue A (pp. 203 – 208) 2014

Xanthine and hypoxanthine: in a search for conical intersections S_0/S_1 connected with deformations of pyrimidine residue of the purine ring

V. B. Delchev*

Department of Physical Chemistry, University of Plovdiv, Tzar Assen 24 str., 4000 Plovdiv, Bulgaria

Received March 19, 2014; Revised April 09, 2014

Dedicated to Acad. Dimiter Ivanov on the occasion of his 120th birth anniversary

The oxo N9H tautomers of xanthine and hypoxanthine were studied theoretically at the CC2/aug-cc-pVDZ level in order to find conical intersections S_0/S_1, which show deformations of the pyrimidine rings. The conical intersections were characterized locally by adiabatic surfaces constructed on the narrow grid. The accessibility of the conical intersections from the excited state was also implied.

Key words: CC2 method, conical intersections, hypoxanthine, xanthine

INTRODUCTION

Xanthine (**XA**) is a purine base, which can be found in most human body tissues. This compound is produced through purine degradation. It is obtained enzymatically from guanine and hypoxanthine (**HXA**) by deamination and oxidation respectively. Hypoxanthine is a naturally occurring deaminated form of adenine. It is obtained as an intermediate in the purine catabolism reaction. It is also included in the anticodon of tRNA as the nucleoside base inosine [1].

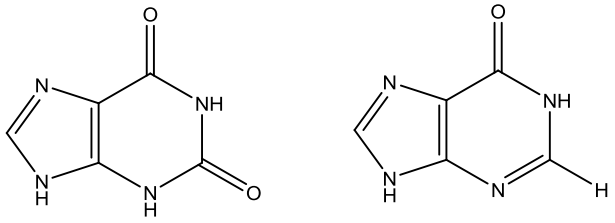

Scheme 1. Canonical structures of xanthine and hypoxanthine N9H tautomers.

The canonical structures of N9H tautomers of xanthine and hypoxanthine are given in Scheme 1. As one can see, hypoxanthine has one extra C=N bond in pyrimidine residue (canonical structure) than xanthine. To our knowledge, the internal conversions of the excited states of pyrimidines and purines occur through a twisting around the double bond(s) within the rings [2-6]. These mechanisms are known to be main channels for a non-radiative decay of the excited states [7,8], which determine their high photostability with respect to UV radiation. Unfortunately for purines, especially for (hypo)xanthine, these reactions are not very well clarified, even though some excited states have been an object of the theoretical research of Farrokhpour *et al.* [9], who have tried to explain the photoelectron spectra of both compounds. However, no information for the excited states' deactivation channels has been given [9]. Some excited-state non-radiative decay paths of xanthine through conical intersections S_0/S_1 have been studied theoretically; however they concern only the imidazole part of the ring [10].

Theoretical calculations and experimental UV spectral investigations have revealed that in aqueous solution the N9H tautomer of hypoxanthine is dominant over the keto-N7H form [11-14]. In the crystalline phase this tautomer is the most stable one either [15]. The keto and enol tautomers, and their stability in aqueous solution have been reported in the paper of Stimson et al [16]. They have been established by UV spectroscopy that in acid solution the enol forms of hypoxanthine and xanthine dominate [16]. Some recent investigations have revealed that hypoxanthine in aqueous solution shows absorption maximum at 250 nm [17]. It was found also that the lifetimes of hypoxanthine in aqueous media are 2.3±0.3 ps (probe 250 nm) and 130±20 fs (probe 570 nm) [17]. The major conclusion of the latter research is that hypoxanthine appears to decay non-radiatively by puckering of the six-membered ring

* To whom all correspondence should be sent:
E-mail: vdelchev@uni-plovdiv.net

in aqueous media. However, a concrete mechanism has not been proposed and commented.

The aim of the reported research is to throw light upon the deformation mechanisms of pyrimidine fragments of xanthine and hypoxanthine and to clarify their contribution to internal conversions S_0/S_1 or fluorescence in both compounds. The study requires a search of accessible and reliable conical intersection(s) mediating the $S_1 \rightarrow S_0$ decay (internal conversion). Such conical intersections and their accessibility could explain the high UV photostability of both compounds. In the cases of excited state decay either internal conversion or fluorescence may dominate. The knowledge which process prevails is important to the understanding of whether the compound could find application as photoprotector or not.

THEORETICAL METHODS

The ground-state equilibrium geometries of the N9H tautomers of xanthine and hypoxanthine were optimized at the CC2 level [18,19]. Their structures were used to calculate subsequently the vertical excitation energies of the minima with no symmetry restrictions.

The emission energies were found with the optimized structures of the excited states (CC2). The optimizations of the excited state equilibrium geometries were carried out using symmetry restrictions - C_S. This approach allows distinguishing of the excited states under consideration by symmetry, which is always useful in the studies of electronic states involving a large number of configurations. Thus, the $^1\pi\pi^*$ excited states have symmetry A', while the $^1n\pi^*$ and $^1\pi\sigma^*$ excited states have symmetry A". The optimizations of the excited states without symmetry restrictions led to a mixing of excited states and the assignment of the states is not always possible.

For the generation of adiabatic structures on the narrow grid around the conical intersections we orthogonalized the vectors **g**=2GD and **h**=DC by the Yarkony's procedure [20]. Further procedure for the PESs' constructions is described in the paper of Woywod [20]. The adiabatic PESs were constructed using the normal modes of the geometry-minimum, as obtained from CASSCF computations [21,22].

All computations were performed at the CC2/aug-cc-pVDZ level with the TURBOMOLE program package [18,23]. Only the optimizations of the conical intersections and the geometries-minima for the adiabatic PESs were performed at the CASSCF(6,6)/6-31G* level with the program GAUSSIAN 03 [24].

RESULTS AND DISCUSSION

Equilibrium geometries

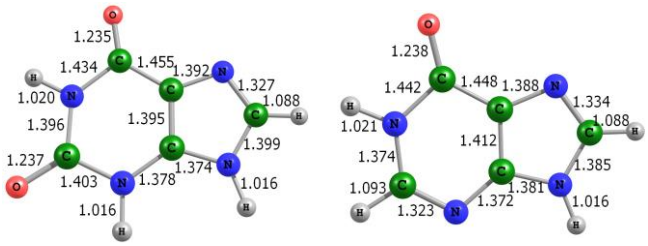

xanthine ***hypoxanthine***

Fig. 1. CC2 ground-state equilibrium geometries of xanthine and hypoxanthine.

The ground-state equilibrium geometries of **XA** and **HXA** found at the CC2 level are illustrated in Fig. 1. The structures are planar which allows using symmetry (C_S) to study the excited states which are vertically located over the ground-state minima. As seen **HXA** has one extra C=N bond in the pyrimidine residue than **XA**. This bond implies twisting around which is usually favored in the excited state than in the ground state.

Vertical excitation and emission energies

Table 1. Vertical excitation and emission energies of xanthine and hypoxanthine.

XA			**HXA**		
State	eV	nm	State	eV	nm
vertical excitation energies					
$^1\pi\sigma^*$	4.918	252	$^1\pi\pi^*$	4.884	254
$^1n\pi^*$	5.080	244	$^1n\pi^*$	5.253	236
$^1\pi\pi^*$	5.297	234	$^1n\pi^*$	5.422	229
$^1\pi\pi^*$	5.821	213	$^1\pi\pi^*$	5.429	229
$^1\pi\sigma^*$	5.827	213	$^1\pi\sigma^*$	5.436	228
emission energies (C_S symmetry)					
$^1\pi\pi^*$ (A')	4.659	266	$^1\pi\pi^*$ (A')	3.574	347
$^1\pi\sigma^*$(A")	4.307	288	$^1\pi\sigma^*$(A")	3.574	248

The calculated vertical excitation energies of the tautomers of both compounds are presented in Table 1. The data show that the bright $^1\pi\pi^*$ excited state of xanthine (at 5.297 eV) is the third excited state (ordered by energy), while it is the lowest excited state in hypoxanthine (at 4.884 eV). That could be explained with the extra oxygen atom, which is present in xanthine as compared to hypoxanthine; such bases with carbonyl groups have $^1n\pi^*$ excited states with lower energies than those of $^1\pi\pi^*$ excited states [8,10,11]. The molecular orbitals under consideration are illustrated in Fig. 2.

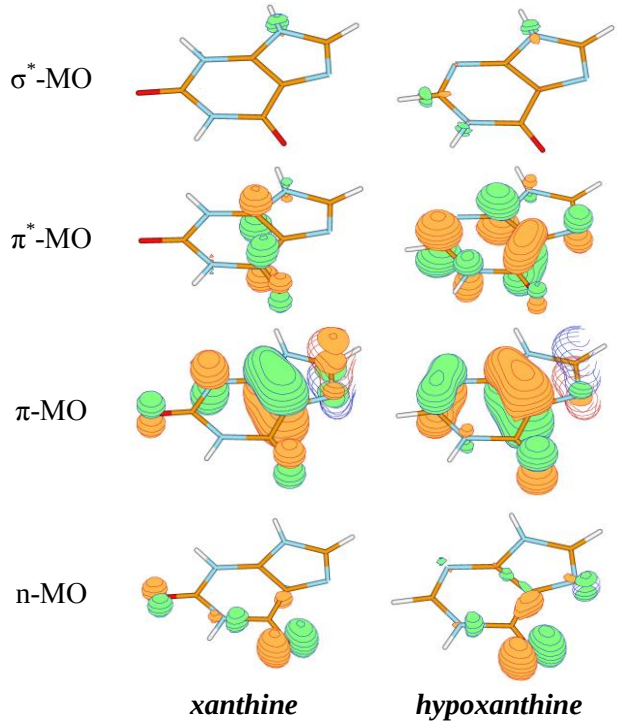

Fig. 2. Selected molecular orbitals involved in the electronic transitions leading to the excited states under consideration.

The calculated $^1\pi\pi^*$ emission energy (in eV) of hypoxanthine is considerably lower than this of xanthine. In other words, the fluorescence maximum of xanthine is expected to be blue-shifted with respect to this of hypoxanthine. To the contrary, the emission energy of the $^1\pi\sigma^*$ excited state (if any maximum of this state can be measured) of xanthine should be red-shifted as compared to hypoxanthine.

Conical intersections

The structures of the optimized conical intersections are illustrated in Fig. 3.

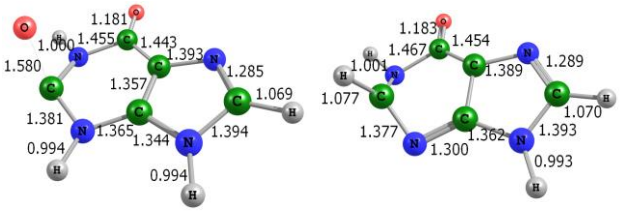

CI_{xa} **CI_{hxa}**

Fig. 3. Conical intersections of xanthine and hypoxanthine obtained through deformations of the pyrimidine residues of purine rings.

They both show deformations in pyrimidine fragment of the purine ring. As seen, the conical intersection S_0/S_1 of **XA** shows deformation of the carbonyl oxygen at the second position (IUPAC). The C=O bond is star-ched to 1.580 Å as compared to the minimum (Fig. 1). The carbonyl oxygen is located in the upper side of the purine ring.

The optimized intersection S_0/S_1 of **HXA** shows a typical twisting of the C=N bond of pyrimidine ring. As expected, this twisting is accompanied by a deviation of the hydrogen atom of the nearest carbon atom out of the molecular plane.

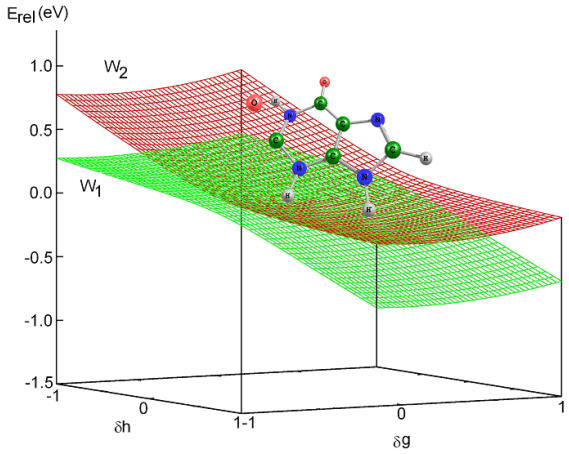

(a)

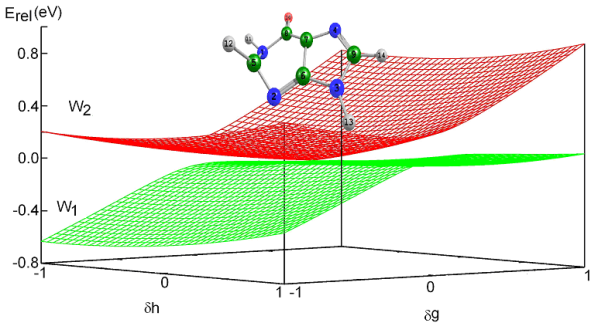

(b)

Fig. 4. Adiabatic potential energy surfaces of the electronic states S_0 (W_1) and S_1 (W_2) of a) xanthine and b) hypoxanthine.

The adiabatic surfaces W_1 and W_2 of the electronic states S_0 and S_1 are presented in Fig. 4. As seen in both cases, for **XA** and **HXA**, the two electronic states are degenerated in the point 0/0: the conical intersection S_0/S_1 is located there. The slope of the S_0-surface after the conical intersection is indicative enough for the course of the reaction since it shows in which direction the reaction could proceed. In other words, the steeper the slope, the higher probability for the reaction to proceed. The S_0-surface of **XA** shows the steepest slope in the direction 1/-1 (these are the end values of δg and δh correspondingly). The S_0-surface of **HXA** indicates the steepest slope in the direction -1/-1.

Energy-level diagrams

In Fig. 5 are depicted the energy-level diagrams and the possible pathways (dashed arrows) of the deactivation processes of the excited states as well as the basic optical transitions (full arrows).

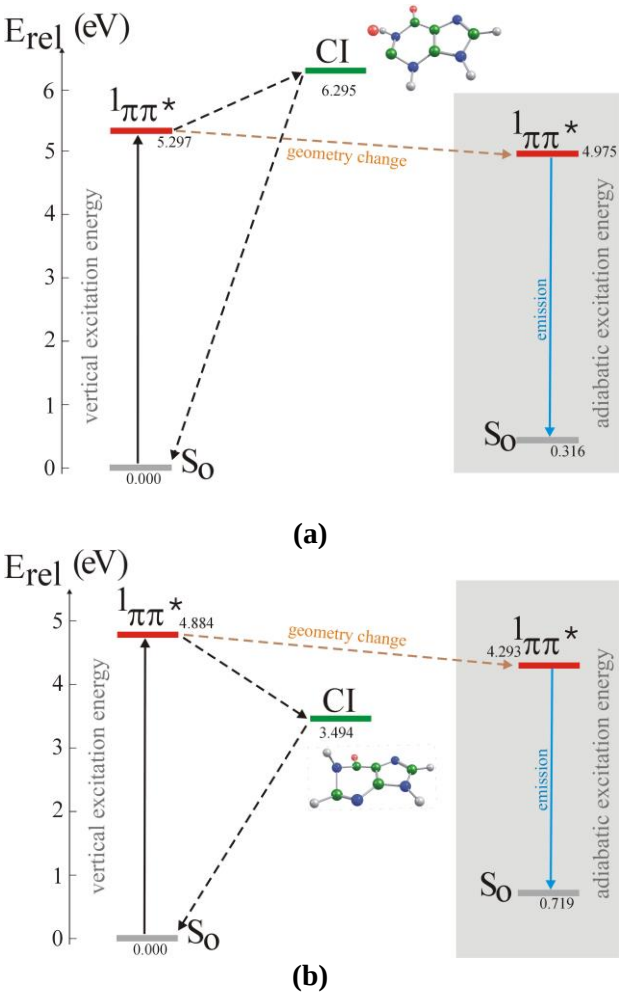

Fig. 5. Energy-level diagrams of the possible deactivation pathways of the N9H tautomers of a) xanthine and b) hypoxanthine – CC2/aug-cc-pVDZ level (gas phase).

As seen, the conical intersection S_0/S_1 of **XA** has higher energy than the energy of the spectroscopically active $^1\pi\pi^*$ excited state. In other words, this conical intersection is not accessible through the lowest bright state. The second bright $^1\pi\pi^*$ excited state of **XA** (Table 1) has lower energy either than the energy of the conical intersection S_0/S_1. As seen from Fig. 5a, the $^1\pi\pi^*$ excited state equilibrium geometry is of lower energy than the vertical excitation energy of this state. It indicates a Stokes shift of 0.638 eV between absorption and fluorescence energies. The experiment has shown fluorescence maximum at 435 nm but in strong acid media (pH=1) [25]. This value is not directly comparable to the calculated one here since, as it was mentioned in the introduction section, it can be associated with the enol tautomer, which is dominant at pH=1 [16]. At pH=7.2 the fluorescence is about 325 nm [26]. Obviously, the fluorescence maximum is approaching the predicted here value despite the fact that the calculations are referred to molecules in the gas phase.

Fig. 5b shows the energy-level diagram of **HXA**. The picture shows that the conical intersection S_0/S_1 has lower energy than the lowest bright $^1\pi\pi^*$ excited state, and thus it can be accessed through this state and a proper excited-state decay path. Our future research will be dedicated to a search of such path connecting both stationary points on the W_2-adiabatic-PES of **HXA**. Perhaps, this conical intersection could be also accessed from the equilibrium geometry of the $^1\pi\pi^*$ excited state, whose energy is lower (the gray area of the picture).The results imply a Stokes shift of 1.31 eV between absorption and fluorescence maxima.

CONCLUSION

The oxo N9H tautomers of xanthine and hypoxanthine were studied theoretically at the CC2/aug-cc-pVDZ level in order to find conical intersections S_0/S_1 which correspond to deformations of the pyrimidine fragment of the purine ring. The energies of the conical intersections and the minima were summarized in energy-level diagrams which shed light upon the possible deactivation channels of the two compounds. It was shown that the conical intersection S_0/S_1 of **XA** cannot be accessed through the spectroscopically active $^1\pi\pi^*$ excited state. Obviously, with respect to these mechanisms only fluorescence is expected; in other words the compound does not exhibit photoprotective properties. To the contrary, the conical intersection S_0/S_1 of **HXA** could be easily accessed through the lowest bright active $^1\pi\pi^*$ excited state of the compound. The domination of the internal conversion of **HXA** shows that the compound can exhibit photoprotective properties. We found also that **HXA** should show larger Stokes shift than **XA** between the absorption and fluorescence maxima.

Acknowledgements: *The author thanks prof. Petko Ivanov (Institute of Organic Chemistry – Bulgarian Academy of Sciences) for the given computational quota and the technical support of the CC2 calculations (Linux-cluster MADARA), Project RNF01/0110.*

REFERENCES

1. J. M. Berg, J. L. Tymoczko, L. Stryer, Biochemistry (5th ed.), W. H. Freeman, New York, 2002.
2. K. A. Kistler, S. Matsika, *J. Chem. Phys.*, **128**, 215102 (2008).
3. S. Matsika, P. Krause, *Annu. Rev. Phys. Chem.*, **62**, 621 (2011).
4. S. Matsika, *J. Phys. Chem. A*, **108**, 7584 (2004).
5. S. Yamazaki, W. Domcke, A. Sobolewski, *J. Phys. Chem. A*, **112**, 11965 (2008).
6. S. Yamazaki, W. Domcke, *J. Phys. Chem. A*, **112**, 7090 (2008).
7. C. Canuel, M. Mons, F. Piuzzi, B. Tardivel, I. Dimicoli, M. Elhanine, *J. Chem. Phys.*, **122**, 074316 (2005).
8. V. B. Delchev, A. L. Sobolewski, W. Domcke, *Phys. Chem. Chem. Phys.*, **12**, 5007 (2010).
9. H. Farrokhpour, F. Fathi, *J. Comput. Chem.*, **32**, 2479 (2011).
10. S. Yamazaki, A. L. Sobolewski, W. Domcke, *Phys. Chem. Chem. Phys.*, **11**, 10165 (2009).
11. M. Shukla, J. Leszczynski (ed.), Radiation induced molecular phenomena in nucleic acids: a comprehensive theoretical and experimental analysis, Springer, 2008.
12. M. K. Shukla, J. Leszczynski, *J. Phys. Chem. A*, **104**, 3021 (2000).
13. M. K. Shukla, J. Leszczynski, *J. Mol. Struct. (Theochem)*, **529**, 99 (2000).
14. B. Hernandez, F.T. Luque, M. Orozco, *J. Org. Chem.*, **61**, 5964 (1996).
15. D. Lichtenberg, F. Bergmann, Z. Neiman, *Isr. J. Chem.*, **10**, 805 (1972).
16. M. M. Stimson, M. A. Reuter, *J. Am. Chem. Soc.*, **65**, 153 (1943).
17. J. Chen, B. Kohler, *Phys. Chem. Chem. Phys.*, **14**, 10677 (2012).
18. C. Hättig, F. Weigend, *J. Chem. Phys.*, **113**, 5154 (2000).
19. C. Hättig, *J. Chem. Phys.*, **118**, 7751 (2003).
20. C. Woywod, W. Domcke, A. L. Sobolewski, H.-J. Werner, *J. Chem. Phys.*, **100**, 1400 (1994).
21. R. H. A. Eade, M. A. Robb, *Chem. Phys. Lett.*, **83**, 362 (1981).
22. H. B. Schlegel, M. A. Robb, *Chem. Phys. Lett*., **93**, 43 (1982).
23. R. Ahlrichs, M. Baer, M. Haeser, H. Horn, C. Koelmel, *Chem. Phys. Lett.*, **162**, 165 (1989).
24. M. J. Frisch, G. W. Trucks, H. B. Schlegel, G. E. Scuseria, M. A. Robb, J. R. Cheeseman, J. A. Montgomery, Jr., T. Vreven, K. N. Kudin, J. C. Burant, J. M. Millam, S. S. Iyengar, J. Tomasi, V. Barone, B. Mennucci, M. Cossi, G. Scalmani, N. Rega, G. A. Petersson, H. Nakatsuji, M. Hada, M. Ehara, K. Toyota, R. Fukuda, J. Hasegawa, M. Ishida, T. Nakajima, Y. Honda, O. Kitao, H. Nakai, M. Klene, X. Li, J. E. Knox, H. P. Hratchian, J. B. Cross, V. Bakken, C. Adamo, J. Jaramillo, R. Gomperts, R. E. Stratmann, O. Yazyev, A. J. Austin, R. Cammi, C. Pomelli, J. W. Ochterski, P. Y. Ayala, K. Morokuma, G. A. Voth, P. Salvador, J. J. Dannenberg, V. G. Zakrzewski, S. Dapprich, A. D. Daniels, M. C. Strain, O. Farkas, D. K. Malick, A. D. Rabuck, K. Raghavachari, J. B. Foresman, J. V. Ortiz, Q. Cui, A. G. Baboul, S. Clifford, J. Cioslowski, B. B. Stefanov, G. Liu, A. Liashenko, P. Piskorz, I. Komaromi, R. L. Martin, D. J. Fox, T. Keith, M. A. Al-Laham, C. Y. Peng, A. Nanayakkara, M. Challacombe, P. M. W. Gill, B. Johnson, W. Chen, M. W. Wong, C. Gonzalez, J. A. Pople, Gaussian 03, Revision D.01, Gaussian, Inc., Wallingford CT, 2004.
25. D. E. Duggan, R. L. Bowman, B. B. Brodie, S. Udenfriend, *Arch. Biochem. Biophys.*, **68**, 1 (1957).
26. M. K. Shukla, P. C. Mishra, *J. Mol. Struct.*, **324**, 241 (1994).

КСАНТИН И ХИПОКСАНТИН: В ТЪРСЕНЕ НА КОНИЧНИ СЕЧЕНИЯ S_0/S_1, СВЪРЗАНИ С ДЕФОРМАЦИЯ НА ПИРИМИДИНОВИЯ ФРАГМЕНТ НА ПУРИНОВИЯ ПРЪСТЕН

В. Б. Делчев

Пловдивски университет "П. Хилендарски", Катедра Физикохимия, ул. Цар Асен 24, 4000 Пловдив, България

Постъпила на 19 март 2014 г.; Коригирана на 9 април 2014 г.

(Резюме)

N9H тавтомерите на оксо ксантина и хипоксантина са изследвани на CC2/aug-cc-pVDZ теоретично ниво с цел да се намерят конични сечения от типа S_0/S_1, за да се изучат механизмите на безизлъчвателна дезактивация на възбудените им състояния, които са свързани с деформации на пиримидиновите остатъци в пуриновите пръстени. Намерените конични сечения са охарактеризирани чрез адиабатните повърхнини на двете електронни състояния S_0 и S_1, построени в ограничено пространство около тях.